Sources of predictability beyond the deterministic limit

Sarah Keeley giving slides by
Franco Molteni
European Centre for Medium-Range Weather Forecasts

Outline

Persistent anomalies in the tropics and extra-tropics: examples from the last two decades

Beyond deterministic predictability in non-linear, chaotic systems: the role of variability in surface conditions and energy/water fluxes

Coupled ocean-atmosphere variability in the tropics and its teleconnections with the extra-tropical flow

Ensemble predictions in the "extended" range: estimates of predictability and actual skill

Predictability on the weekly/monthly time scale arising from sub-seasonal tropical variability and teleconnections

Oct-Dec 1997: floods in East Africa

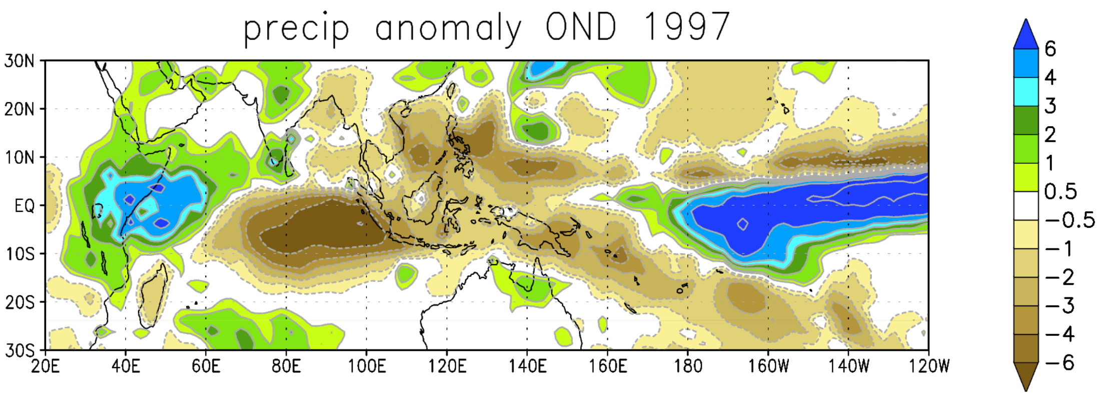

Rift Valley Fever outbreak

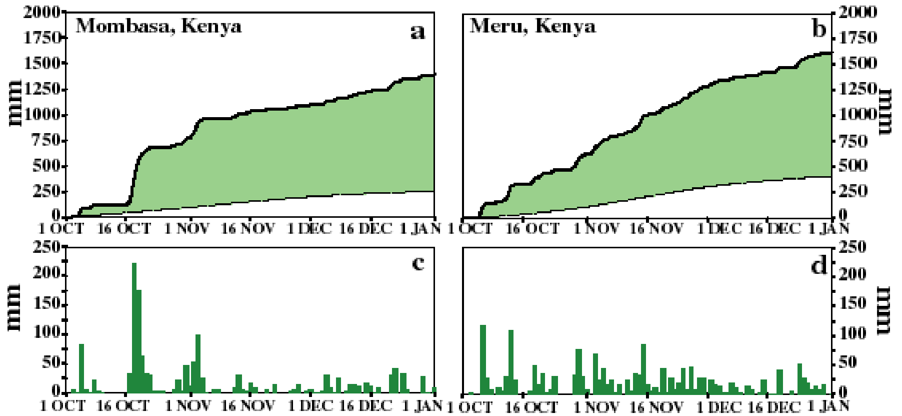

FIG. 45. (a, b) Accumulated observed precipitation (solid curve) and accumulated climatological precipitation (1961–90 base period) (dashed curve) beginning 1 October 1997 and ending 1 January 1998 at (a) Mombasa, Kenya and (b) Meru, Kenya. (c, d) Daily precipitation totals during October 1997–1 January 1998 at (c) Mombasa, Kenya and (d) Meru, Kenya. Green shading in (a)–(b) indicates the difference between the observed and normal accumulated rainfall.

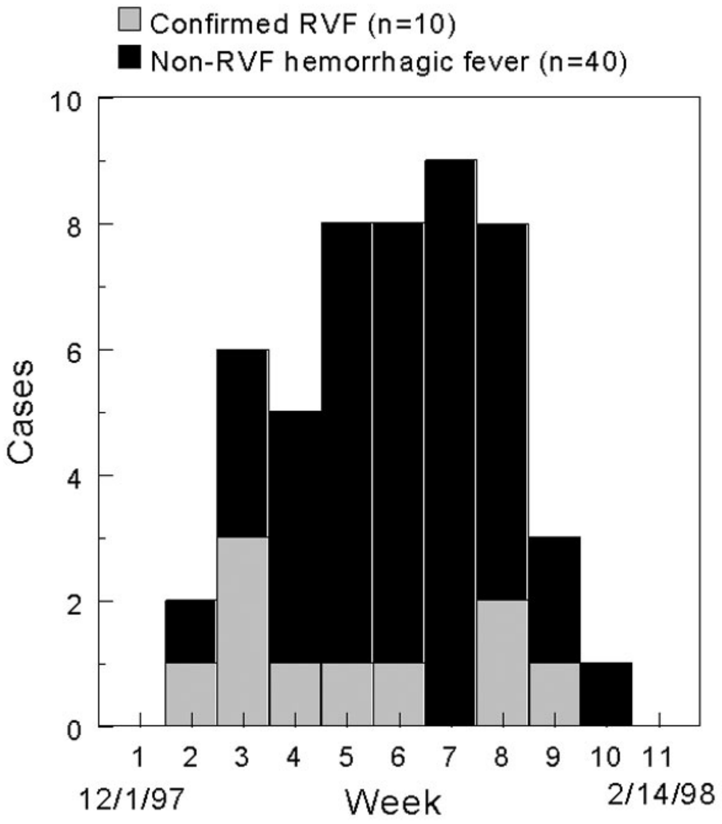

July 2002: drought in India

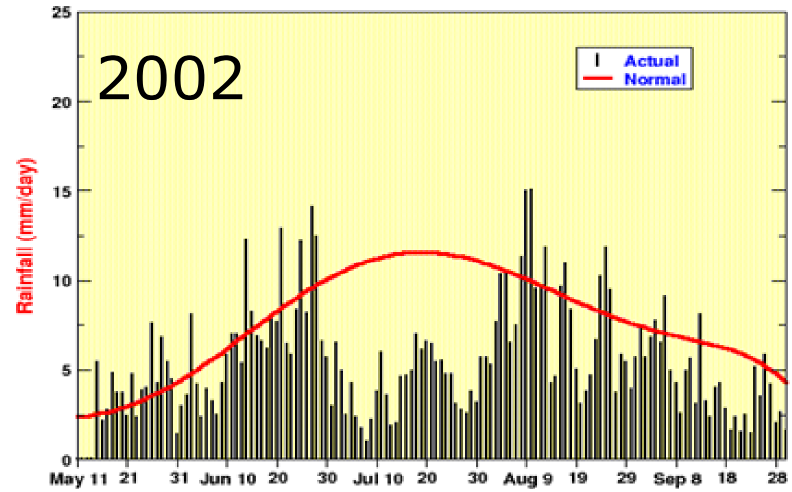

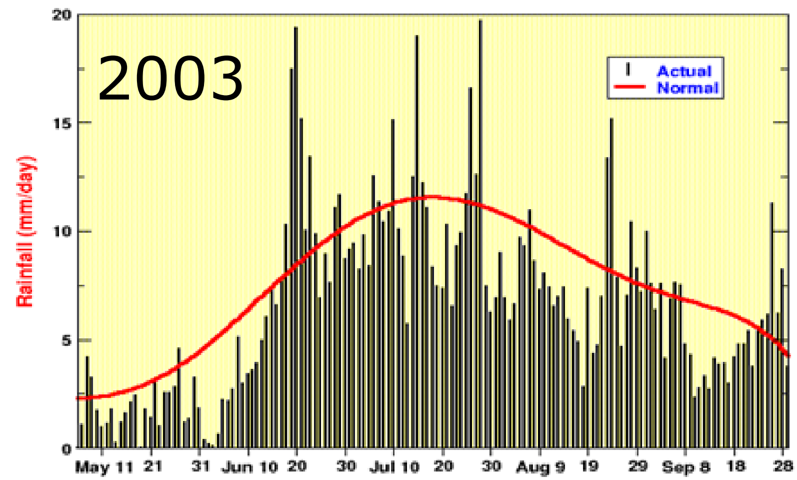

All-India Rainfall time series
May - October

Summer 2003: European heat-wave

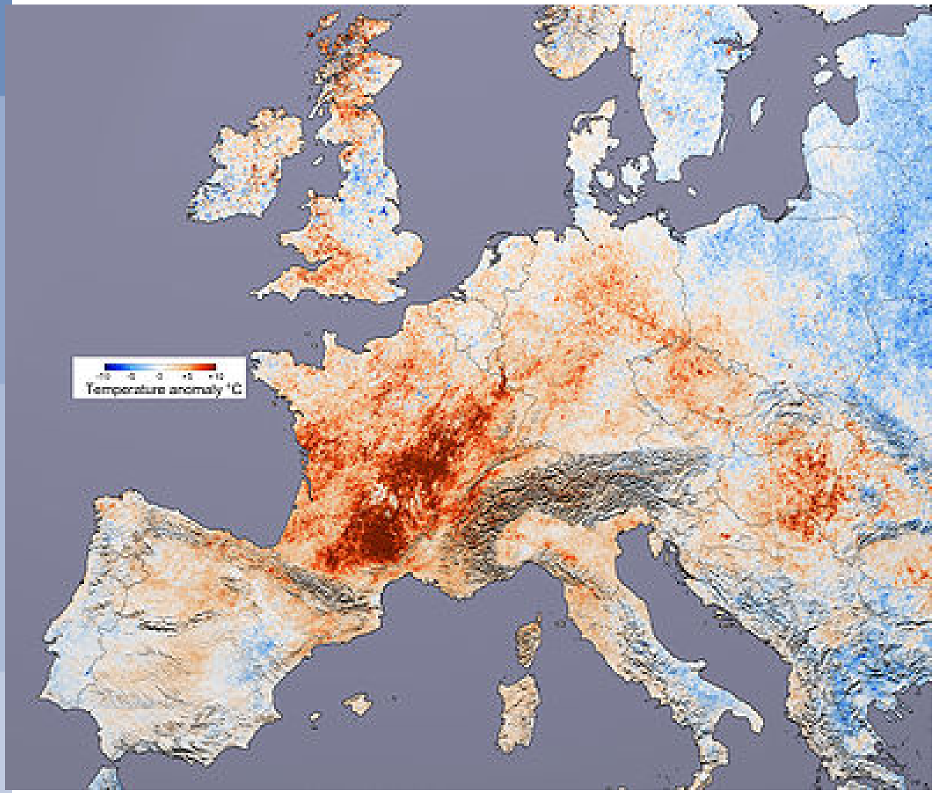

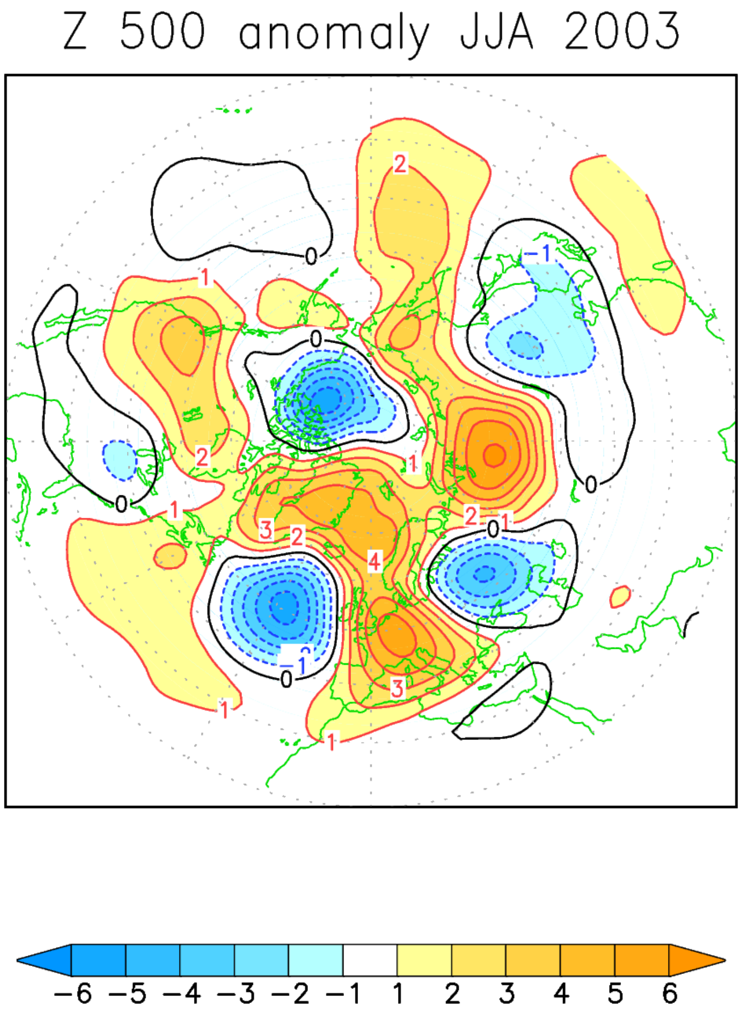

Winter 2009-2010: cold anomaly over N. Europe

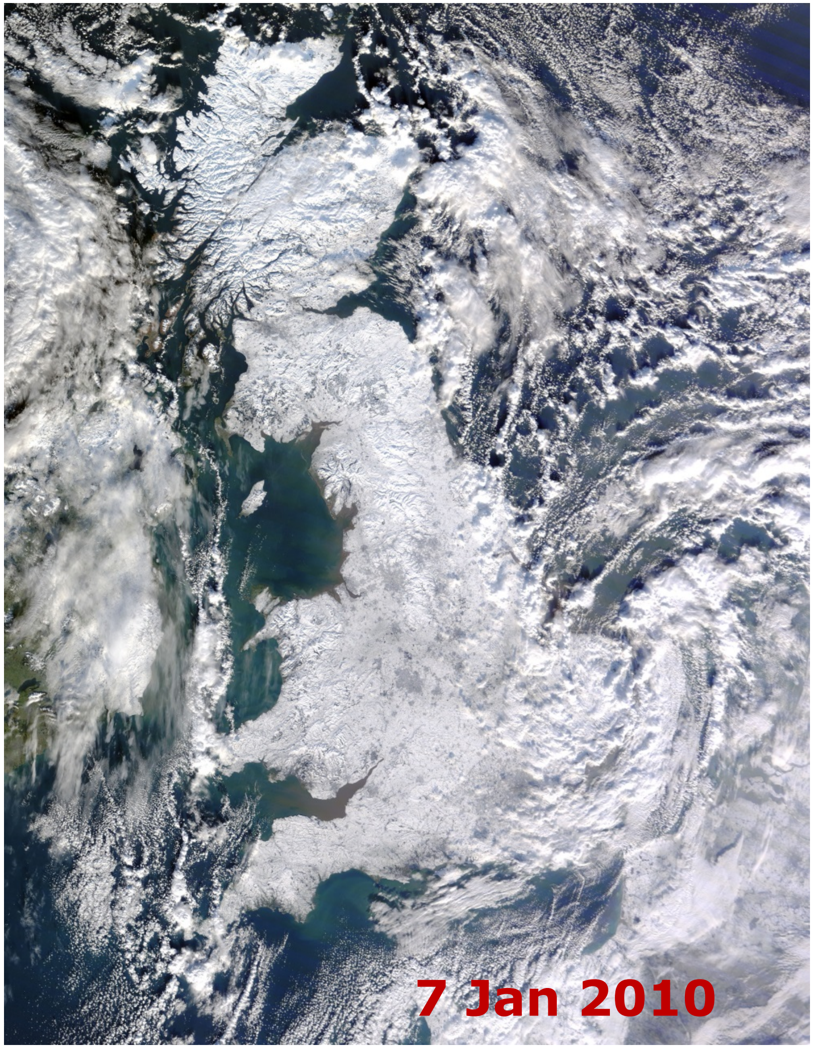

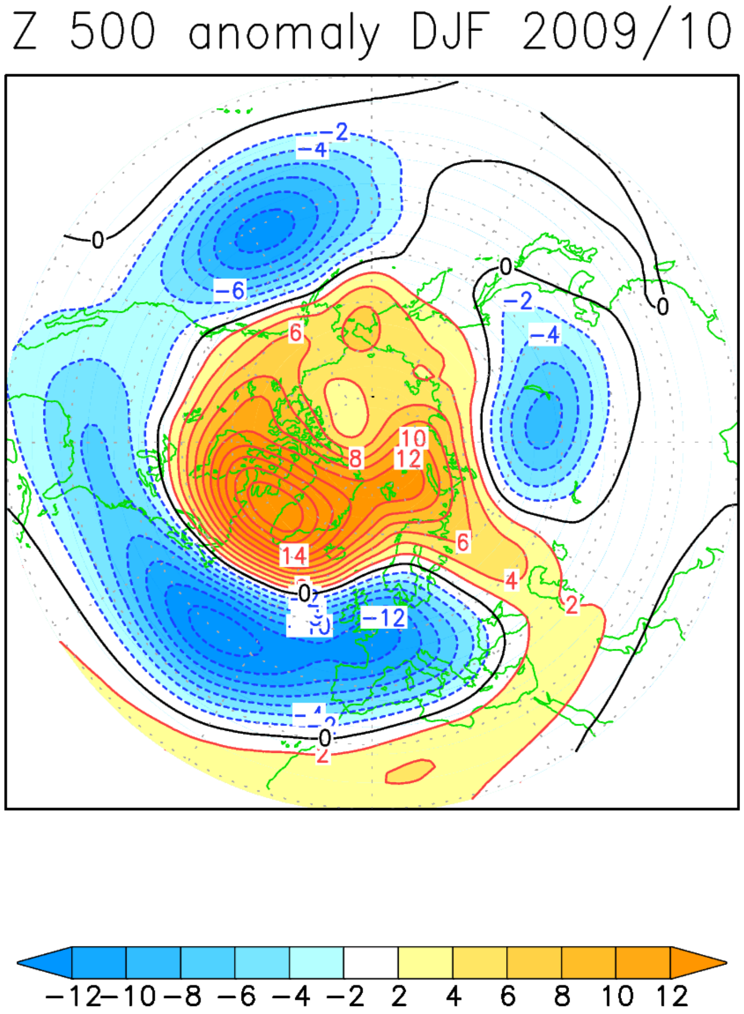

Drought in South-western USA

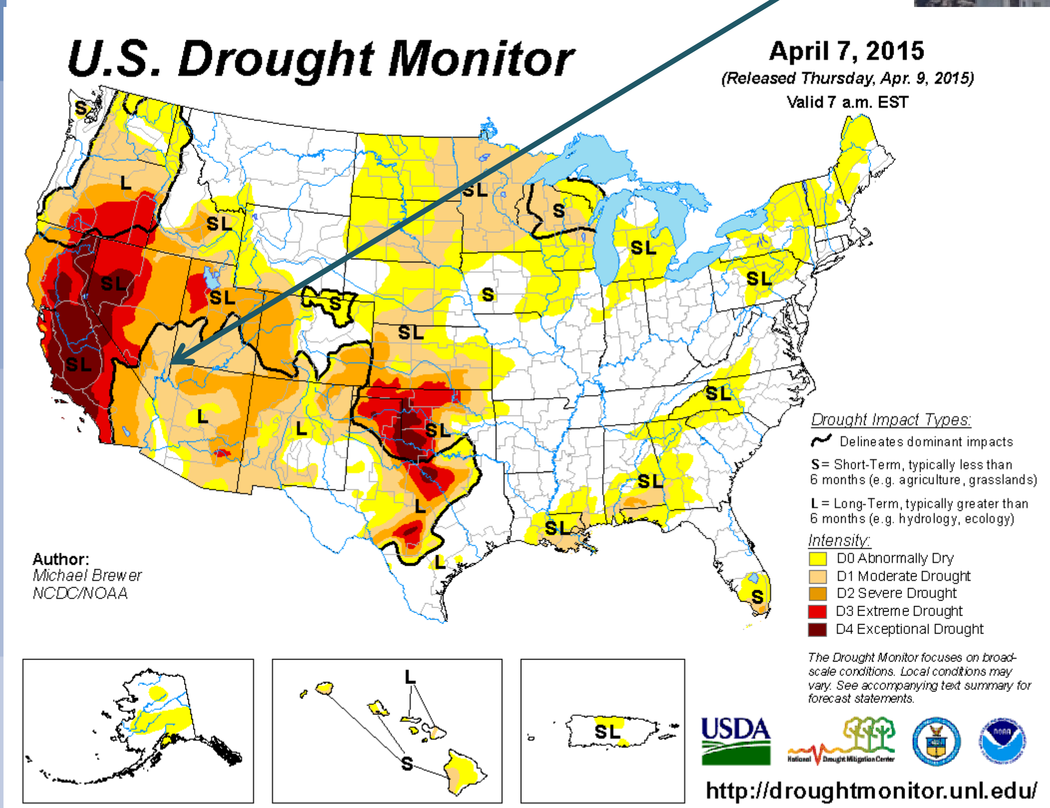

Lake Mead, Colorado River

Lake Mead (Arizona / Nevada) 15-year drought

Chaotic behaviour in non-linear systems

3-variable model of Rayleigh-Benard convection ***(Lorenz 1963)***

$$dX/dt = \sigma\,(Y - X)$$

$$dY/dt = -XZ + \mathbf{r}X - Y$$

$$dZ/dt = XY - bZ$$

Unstable stationary states

$$X = Y = Z = 0$$

$$X = Y = \pm\,[\,b\,(\mathbf{r} - 1)]^{1/2}\ ,\ Z = \mathbf{r} - 1$$

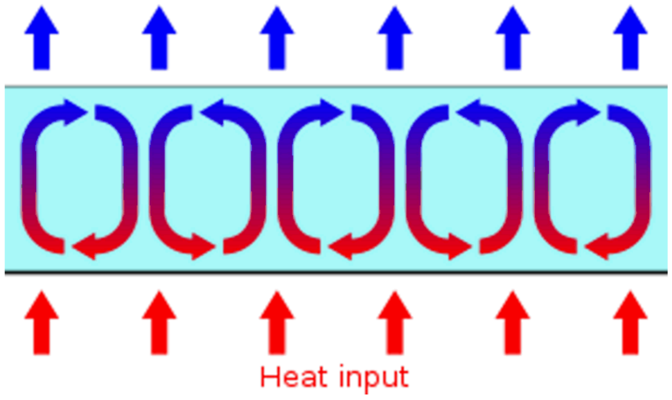

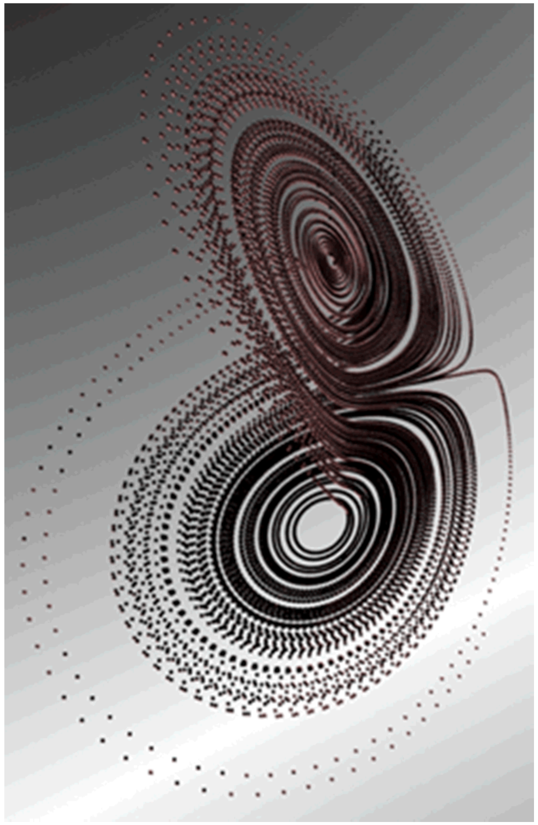

The global energy cycle (2000-2004)

from Trenberth et al. 2009

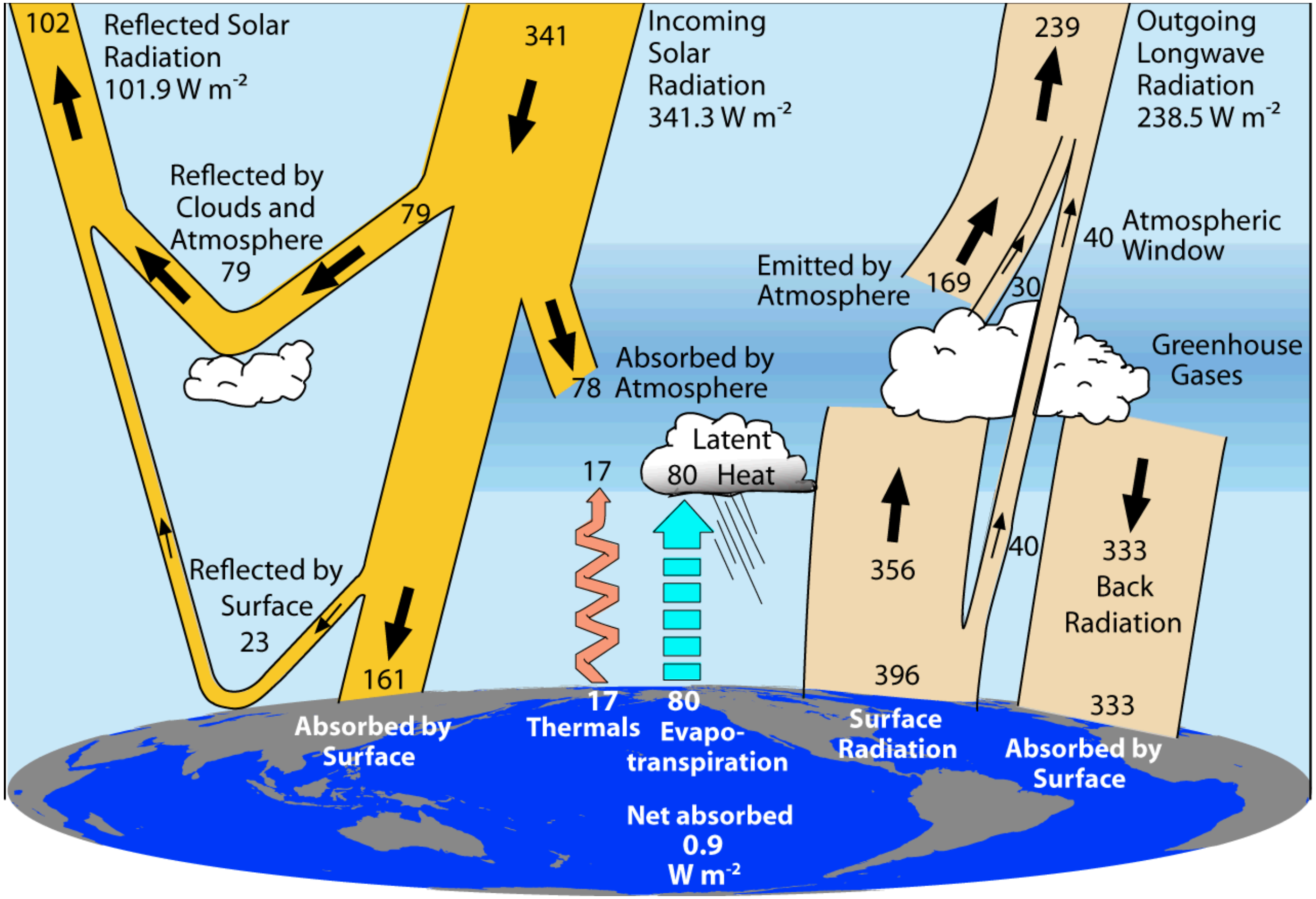

Sea ice: Interaction of climate change and natural variability

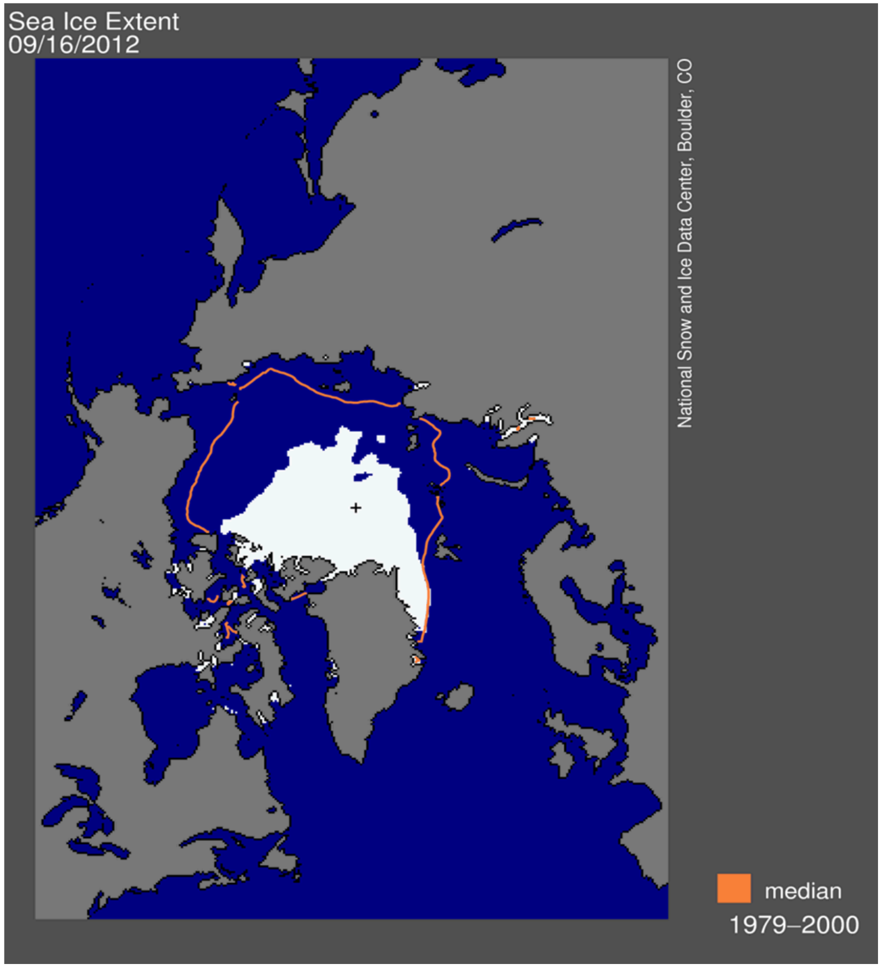

Record minimum in Arctic sea-ice extent: 16/9/2012
(from NSIDC)

El Niño and the Southern Oscillation

Walker and Bliss (1932); Bjerknes (1969)

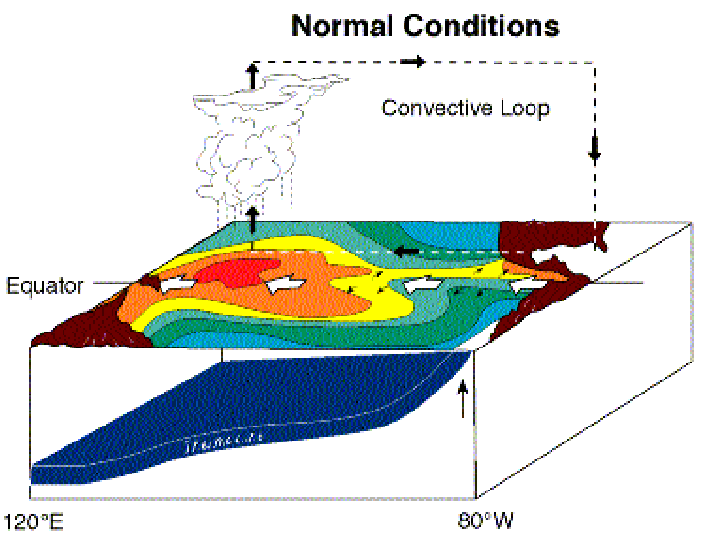

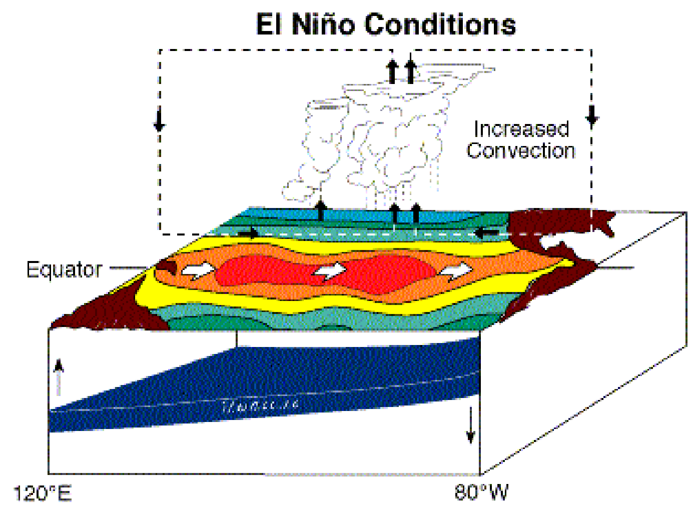

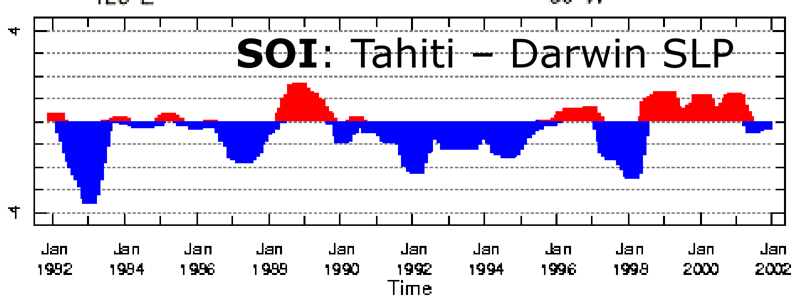

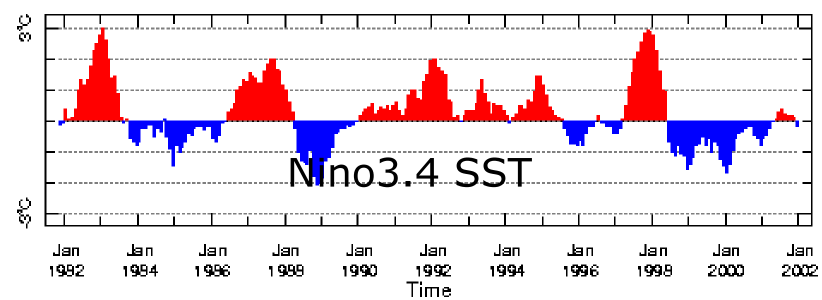

ENSO impacts: rainfall and temperature

WARM EPISODE RELATIONSHIPS DECEMBER - FEBRUARY

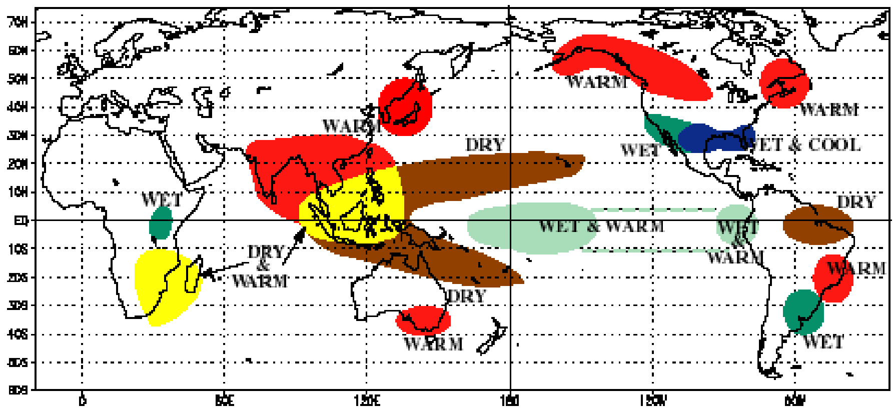

COLD EPISODE RELATIONSHIPS DECEMBER - FEBRUARY

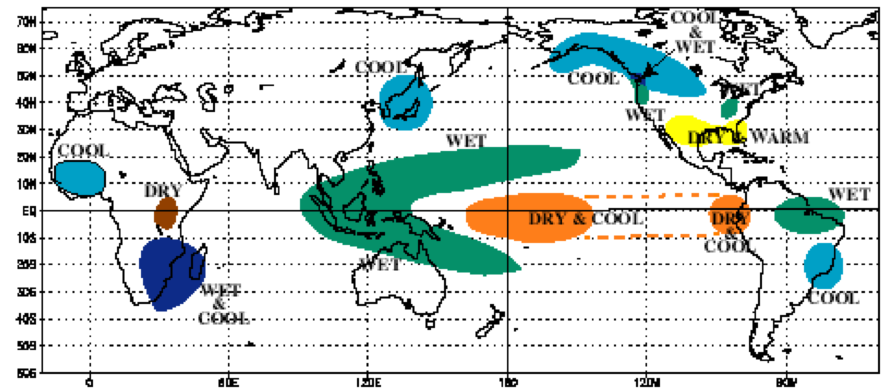

WARM EPISODE RELATIONSHIPS JUNE - AUGUST

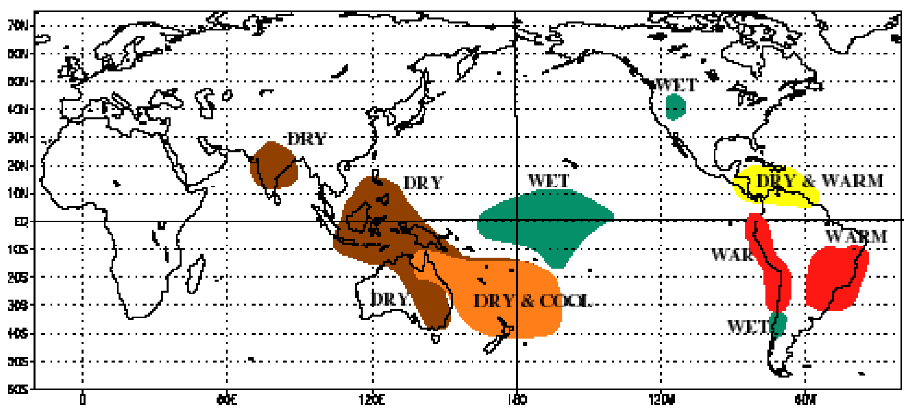

COLD EPISODE RELATIONSHIPS JUNE - AUGUST

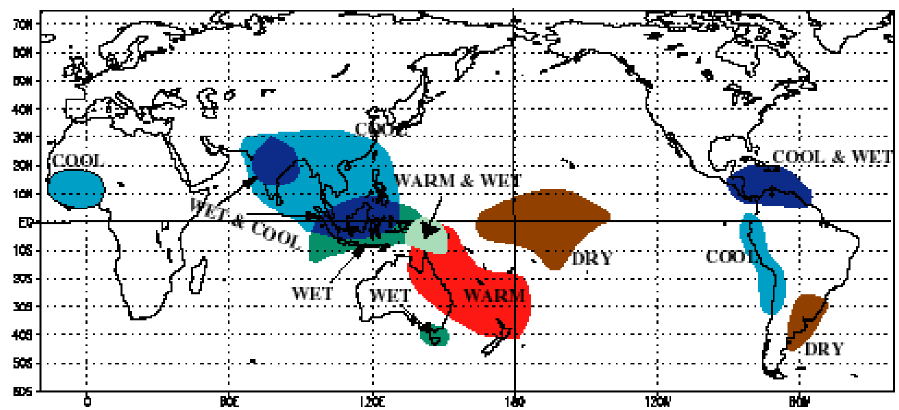

The Indian Ocean Dipole (or I.O. Zonal Mode)

Saji et al. (1999)

Webster et al. (1999)

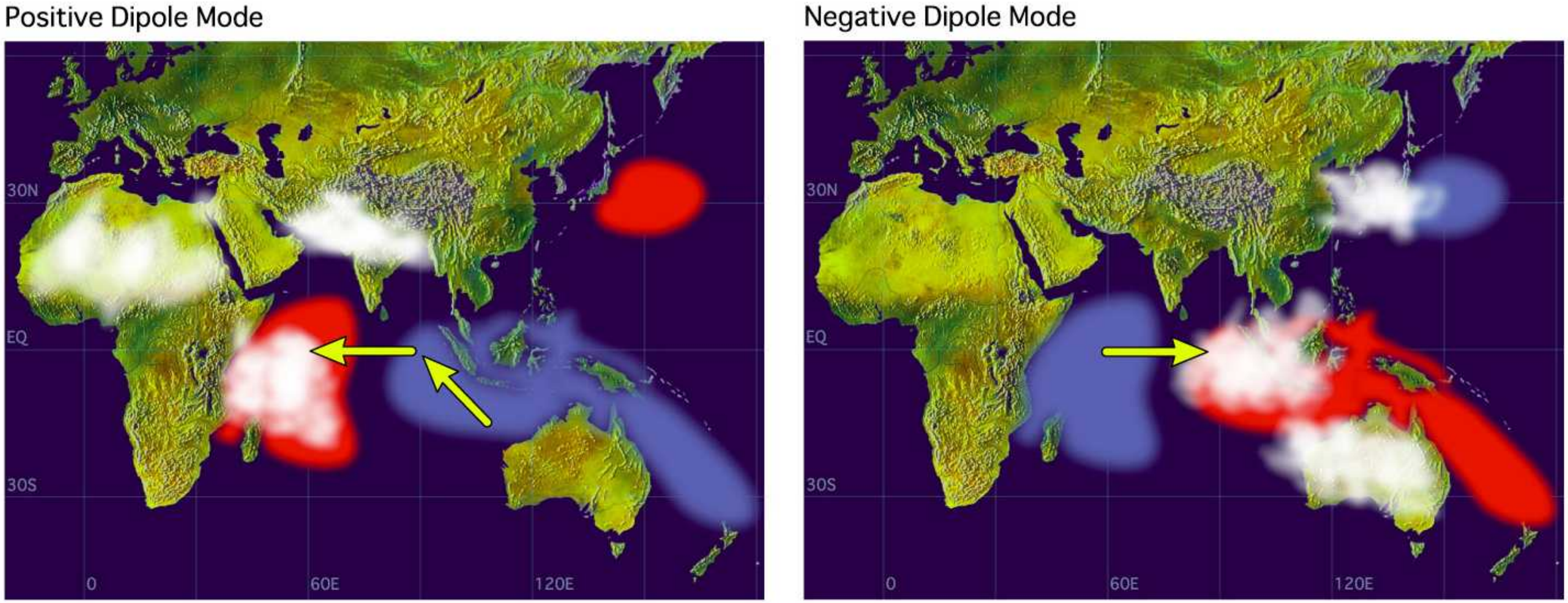

The North Atlantic Oscillation

Walker and Bliss (1932)
Van Loon and Rogers (1978)

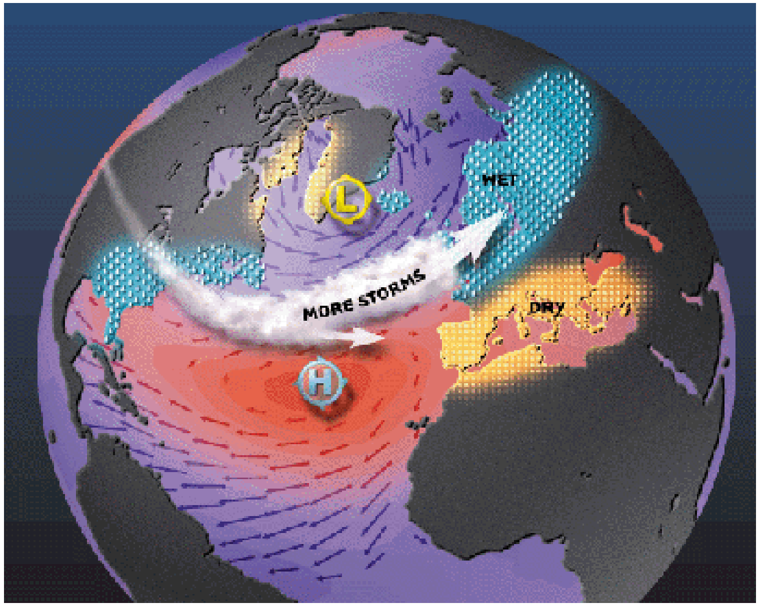

Positive NAO phase

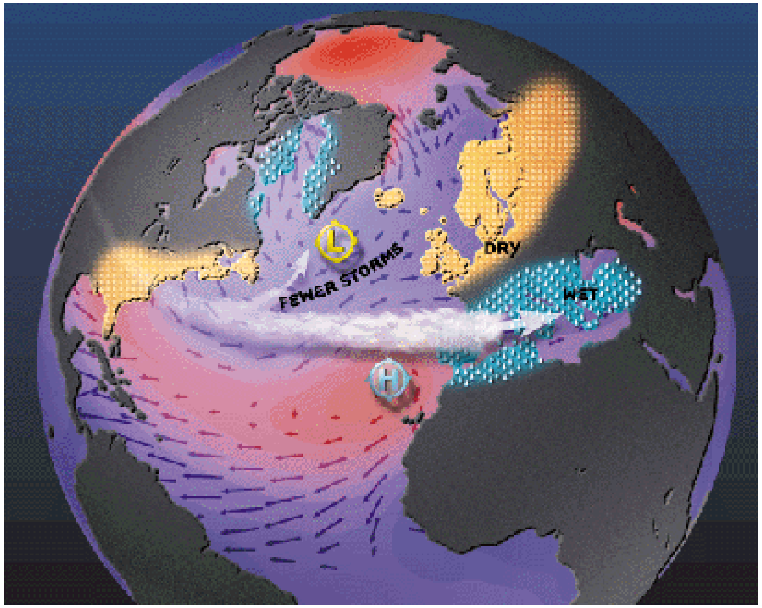

Negative NAO phase

The Pacific /North American (PNA) pattern

500-hPa height composites from Wallace and Gutzler 1981

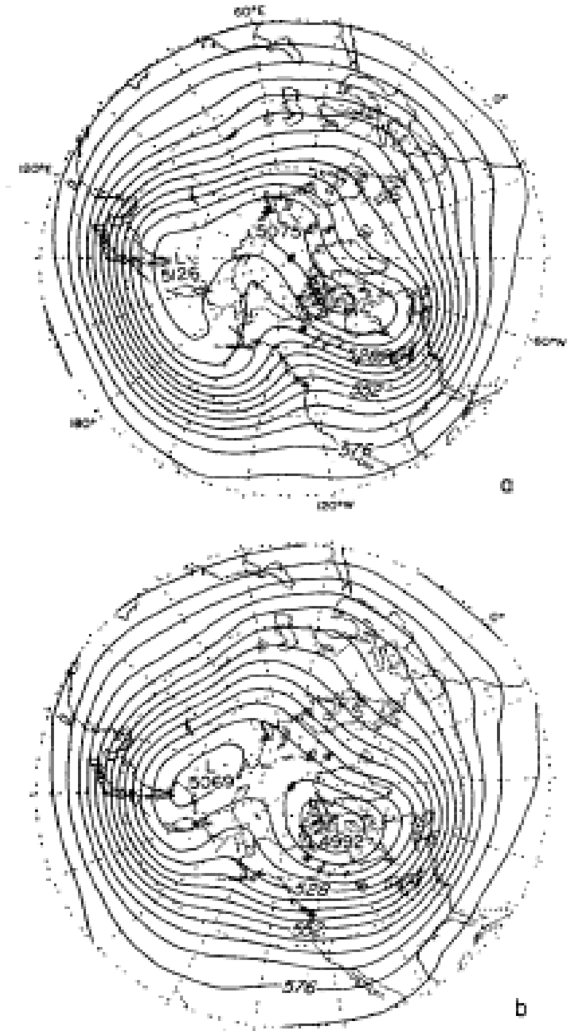

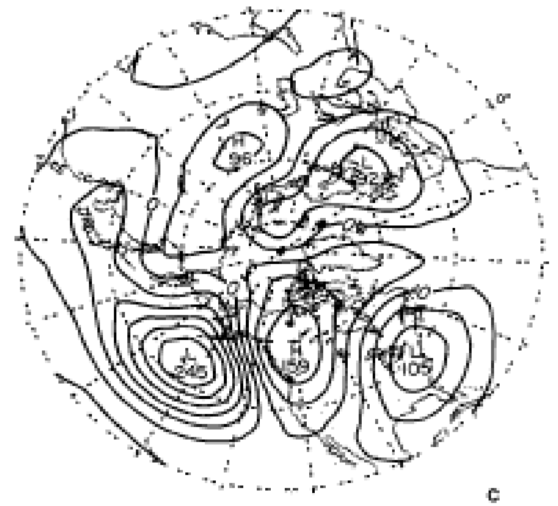

FIG. 17. As in Fig. 13 except for the Pacific/ North American pattern.

Teleconnections with ENSO

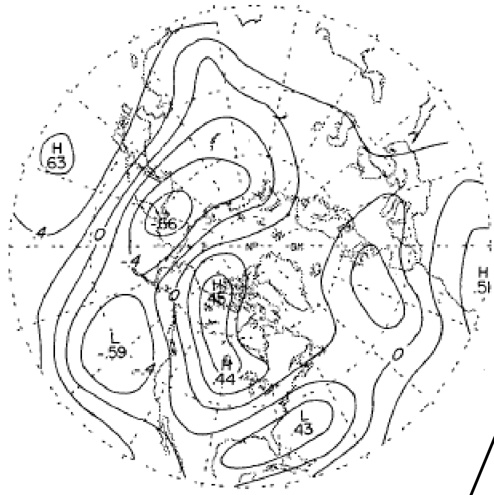

a

Correlation of 700hPa height with
a) PC1 of Eq. Pacific SST
c) SOI index

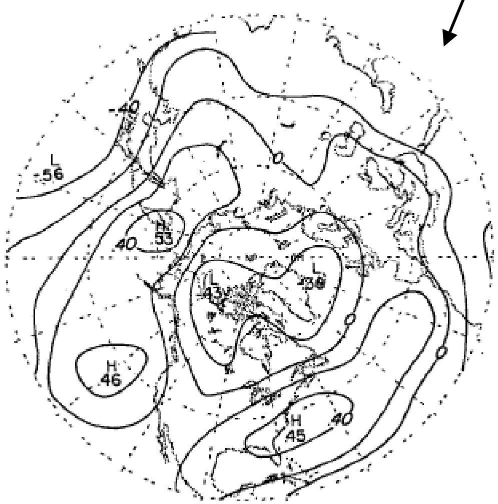

c

Schematic diagram of tropical-extratropical teleconnections during El Niño

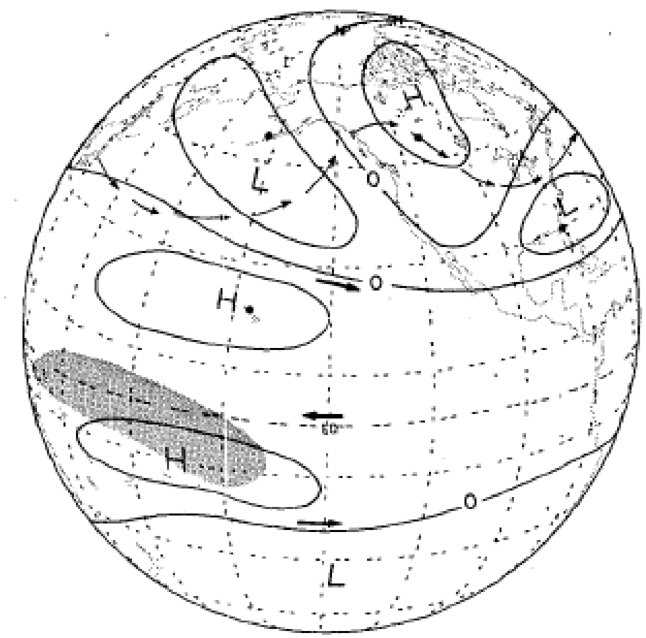

Horel and Wallace 1981

Multiple flow regimes in non-linear models

Charney and DeVore 1979: multiple steady states of a low-order barotropic model with sinusoidal bottom topography

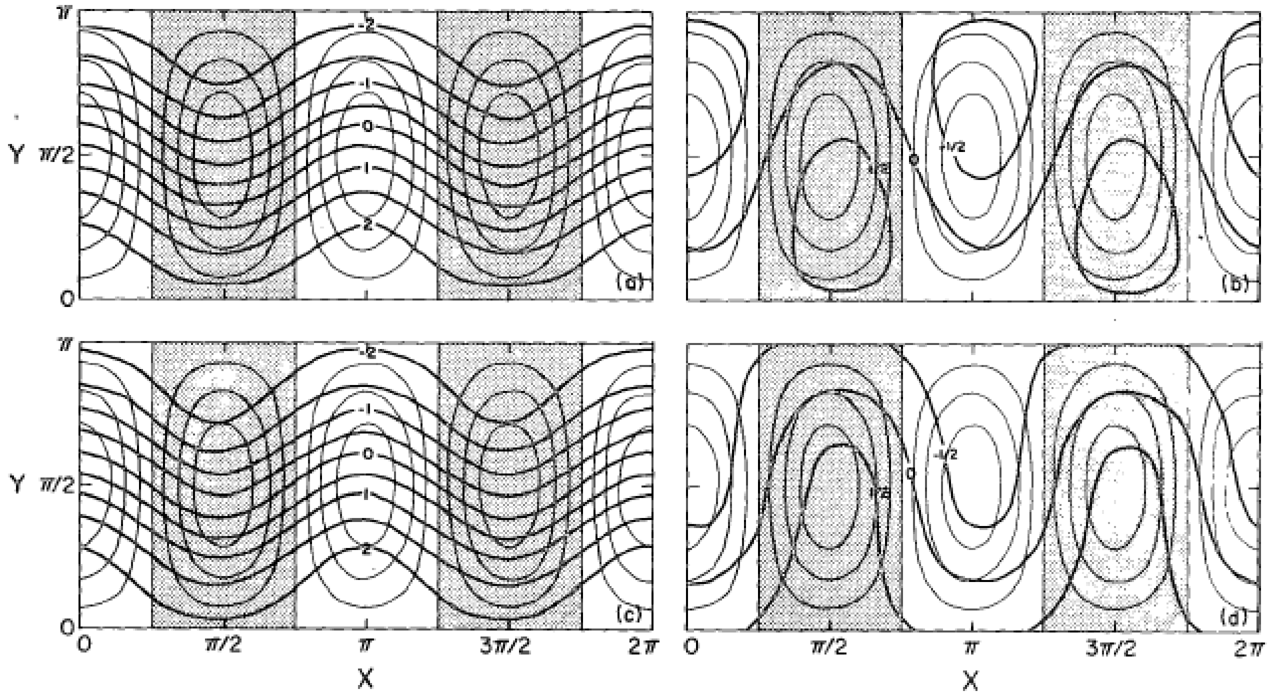

FIG. 4. Streamfunction fields of the stable first mode equilibria of a topographically forced flow for $k = 10^{-2}$, $L/a = ¼$, $n = 2$, $h_0/H = 0.2$ and $\psi_A^* = 0.2$: for the spectral model above resonance (a) and slightly below resonance (b); and for the grid-point model above resonance (c) and slightly below resonance (d). The nondimensional topographic heights are shown with light lines; the contour spacing is 0.05 units, with negative regions shaded.

ECMWF EUROPEAN CENTRE FOR MEDIUM-RANGE WEATHER FORECASTS

The ECMWF Seasonal fc. system (Sys-4)

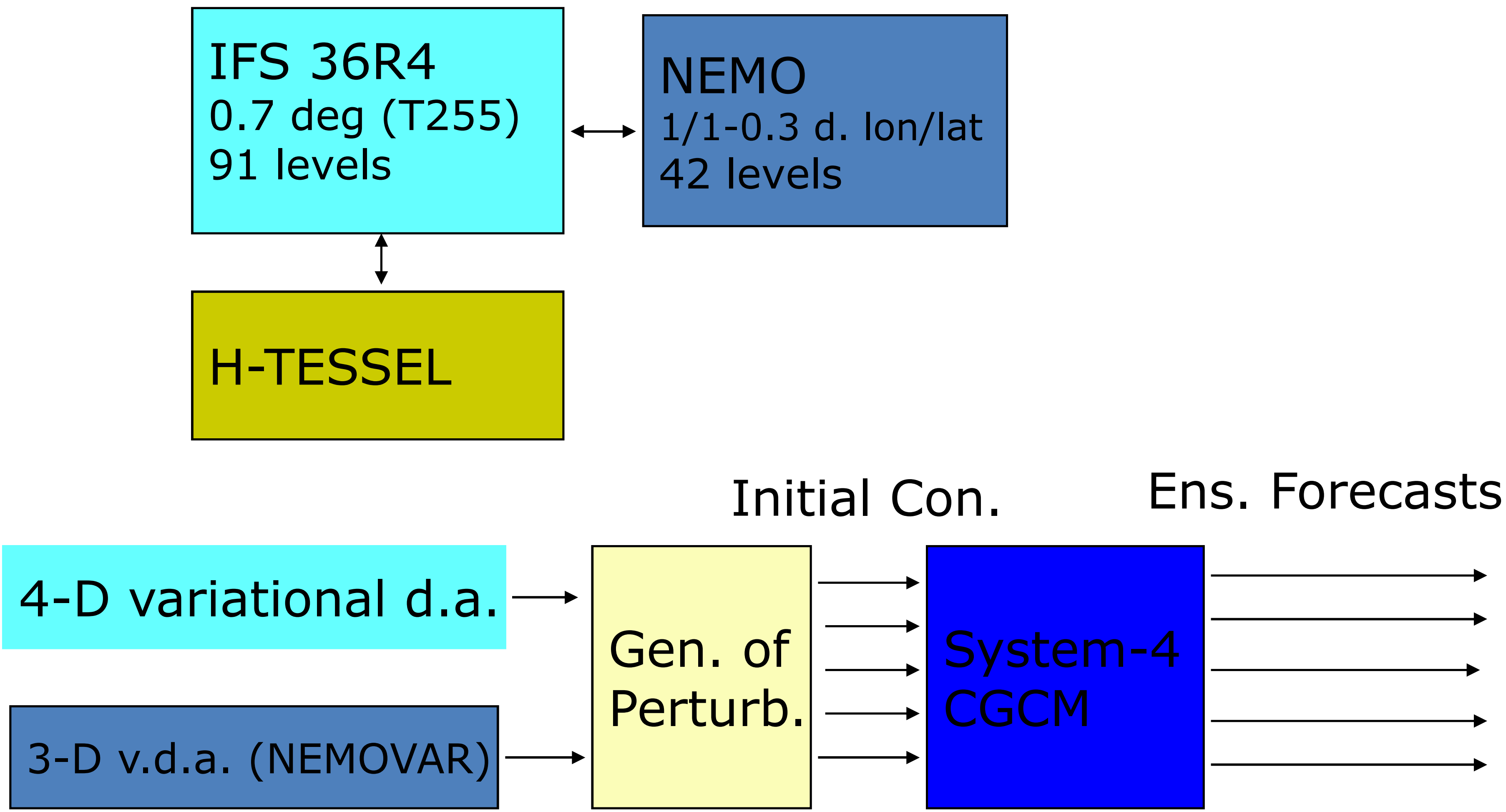

ECMWF System 4: main features

Operational forecasts

51-member ensemble from 1^{st} day of the month

released on the 8^{th}

7-month integration

Experimental ENSO outlook

13-month extension from 1^{st} Feb/May/Aug/Nov

15-member ensemble

Re-forecast set

30 years, start dates from 1 Jan 1981 to 1 Dec 2010

Variability in an ensemble of time-evolving fields

$\boldsymbol{F}\,(t, m) = \boldsymbol{F}\,(t', j, m)$

t' = time within year
$j = 1, N$ (no. of years) $m = 1, M$ (no. of ens. members)

Climatology: $\boldsymbol{F}_{cl}\,(t') = \{\boldsymbol{F}\,(t', j, m)\}_{j,\,m}$
Anomaly: $\boldsymbol{A}\,(t', j, m) = \boldsymbol{F}\,(t', j, m) - \boldsymbol{F}_{cl}\,(t')$

Seasonal mean anomaly: $\boldsymbol{A}_s\,(j, m) = \{\boldsymbol{A}\,(t', j, m)\}_{t'}$
Ens./seas. mean anomaly: $\boldsymbol{A}_{es}\,(j) = \{\boldsymbol{A}\,(t', j, m)\}_{t',\,m}$

- *for an observation/analysis dataset,* ***M =1*** *!*
- *in a "perfect" model environment , the average correlation between $\boldsymbol{A}_{es}$ and $\boldsymbol{A}_s$ is equal to the ratio of their standard deviations.*

Variability of Z 200hPa in DJF from seasonal ensembles

Standard deviation from 11-member ensembles, DJF 1981/2005

5-day means

Seasonal means

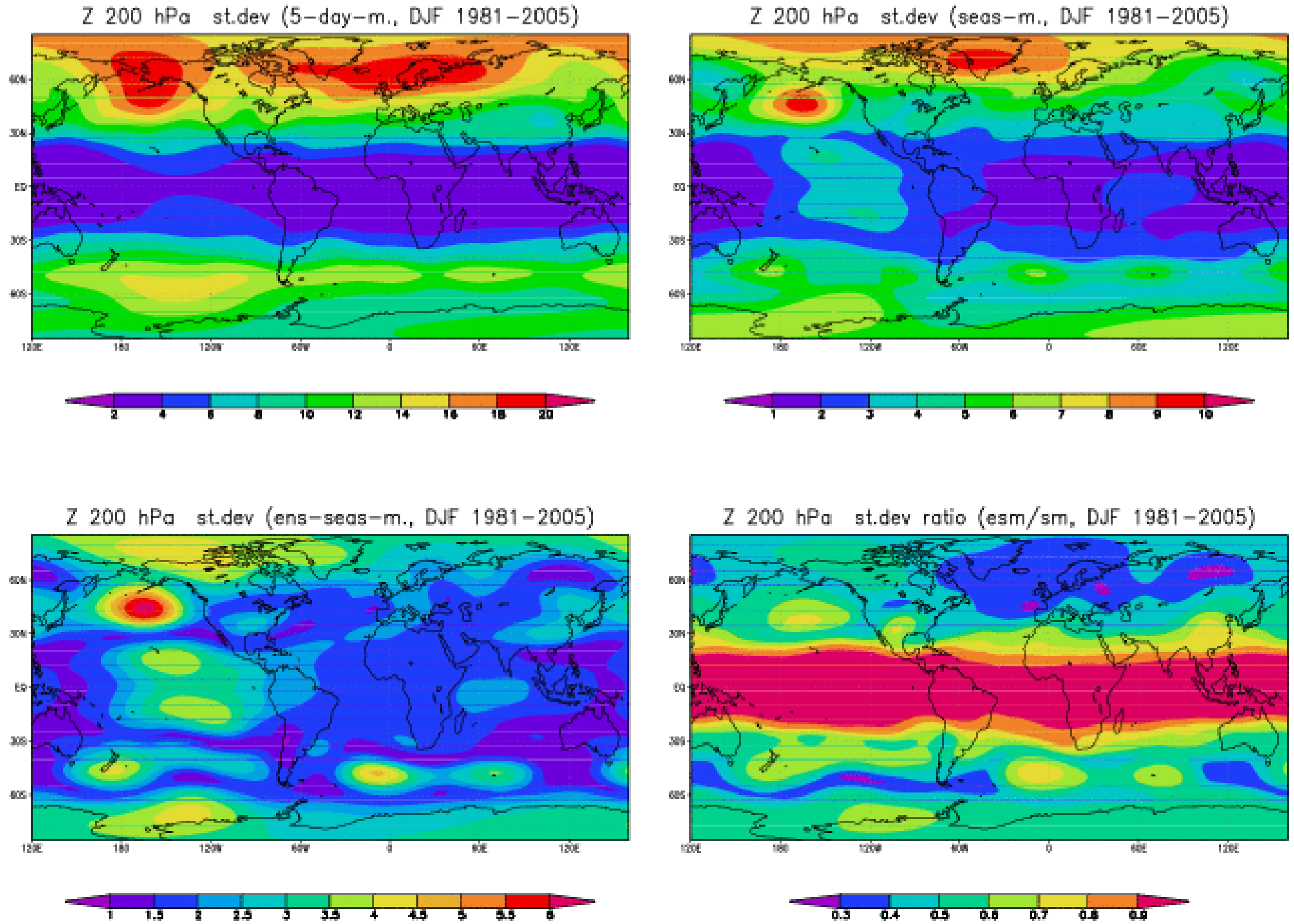

Seasonal - ensemble means

St.dev. ratio

EUROPEAN CENTRE FOR MEDIUM-RANGE WEATHER FORECASTS

Prediction of tropical SST anomalies in Sys4

Nino3.4 DJF

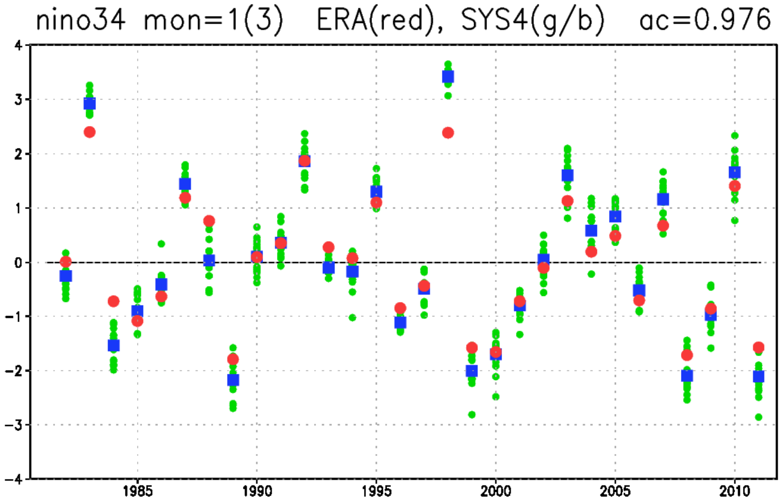

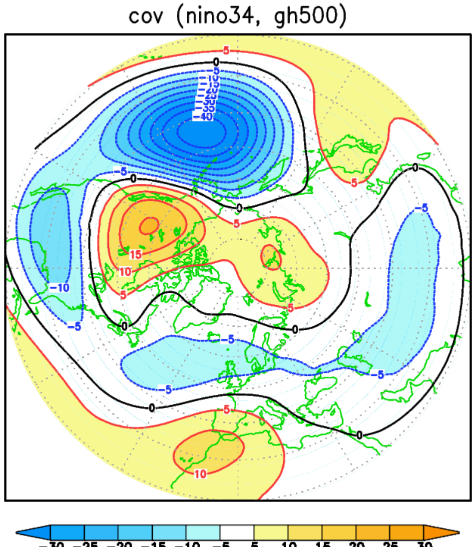

IOD SON

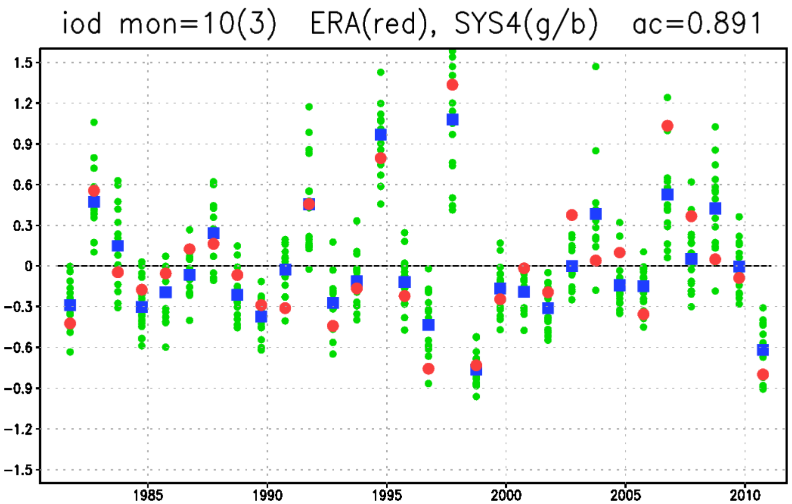

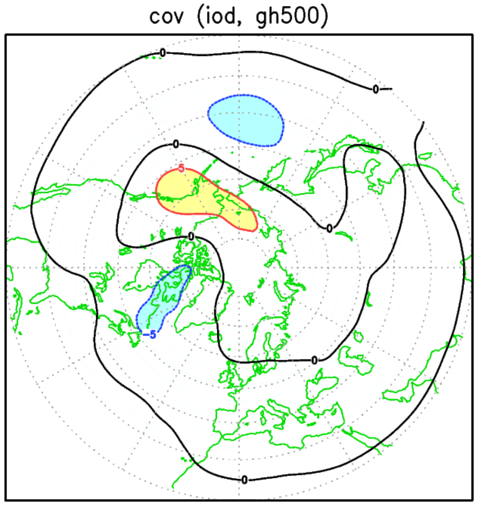

ECMWF EUROPEAN CENTRE FOR MEDIUM-RANGE WEATHER FORECASTS

Prediction of tropical rainfall in Sys4: East Africa (SON)

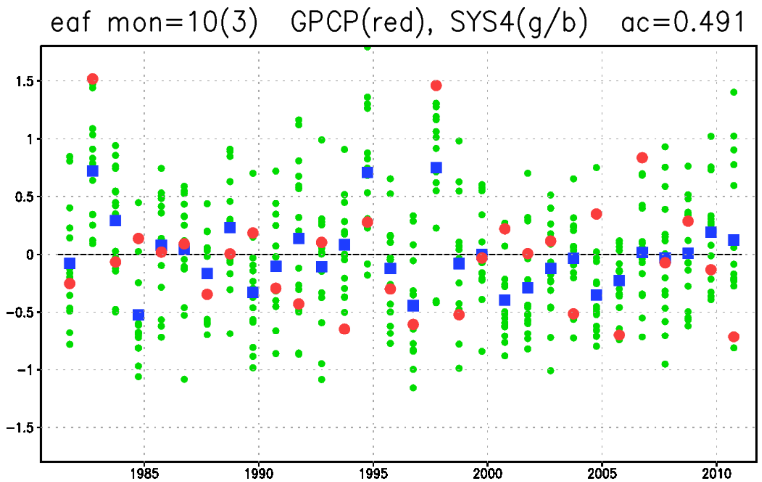

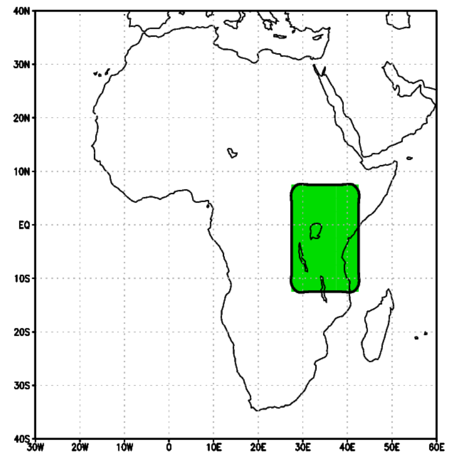

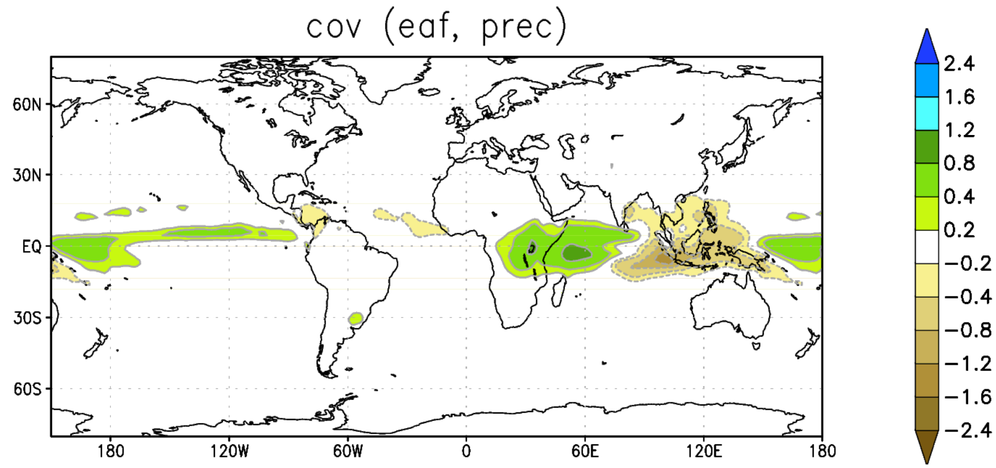

ECMWF EUROPEAN CENTRE FOR MEDIUM-RANGE WEATHER FORECASTS

Prediction of 2-m temperature in Sys4: Europe (DJF, JJA)

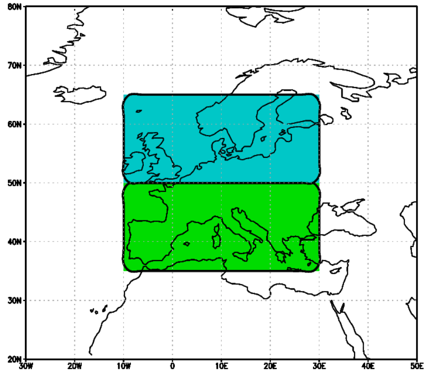

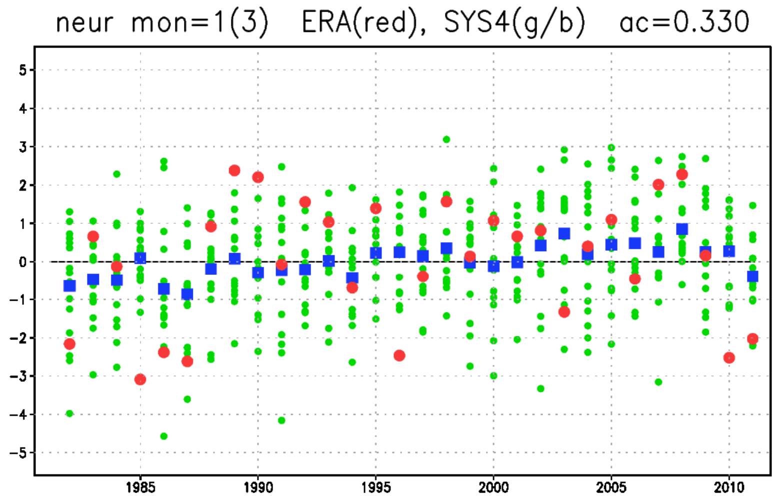

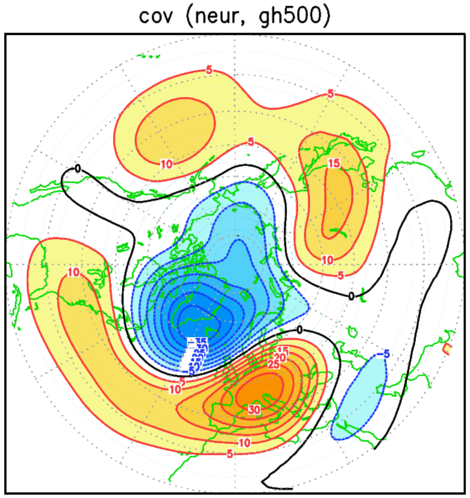

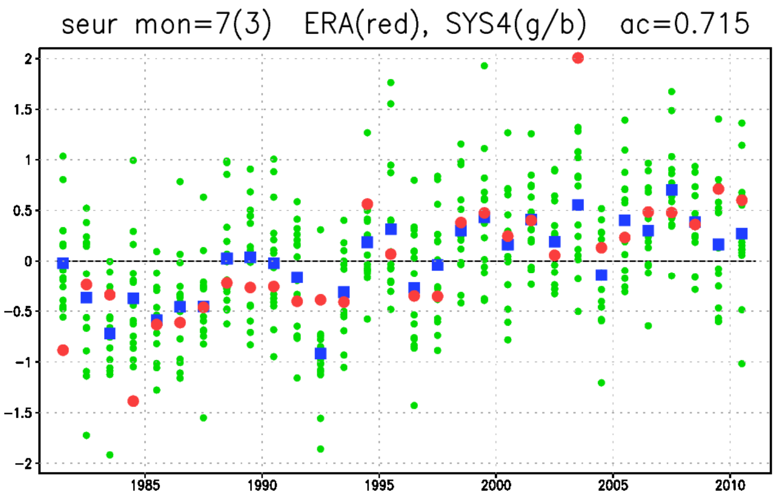

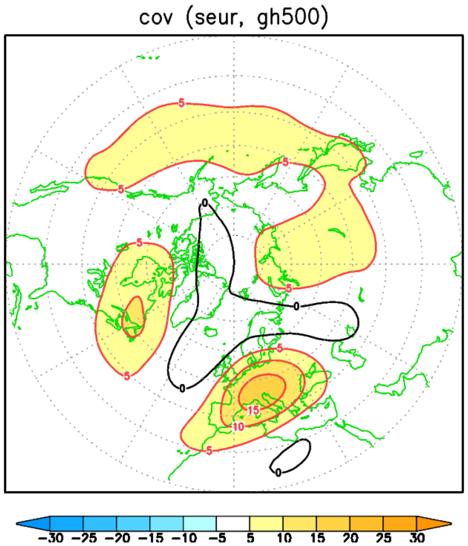

Prediction of 2-m temperature in Sys4: Europe (MAM)

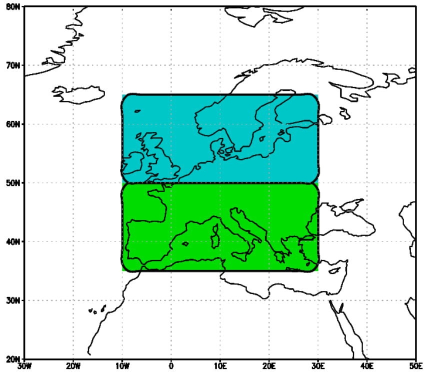

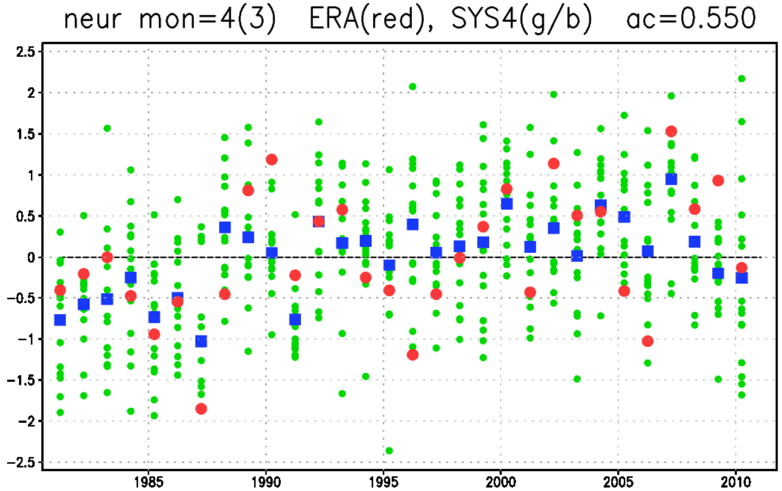

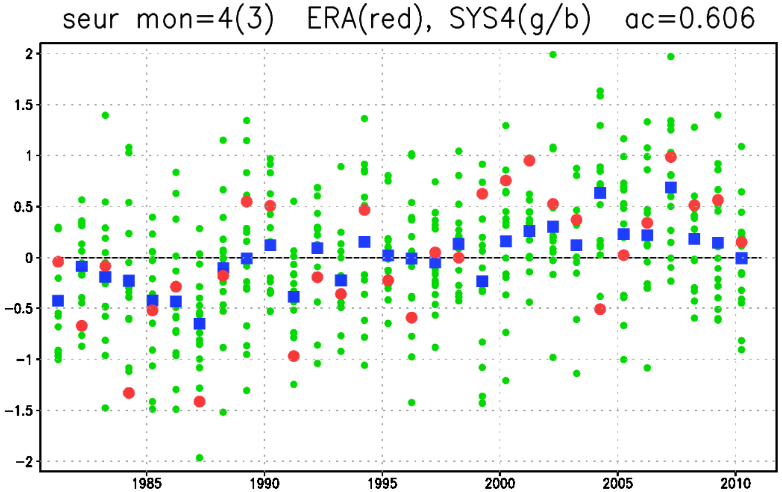

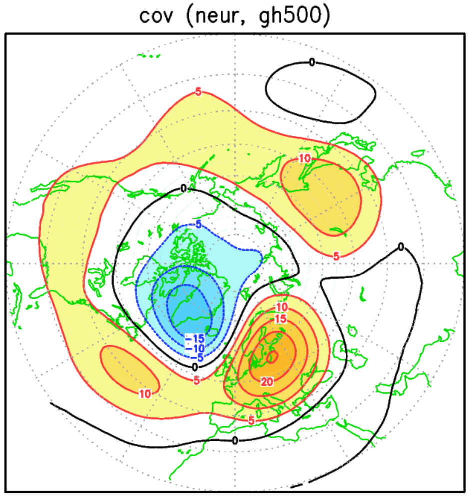

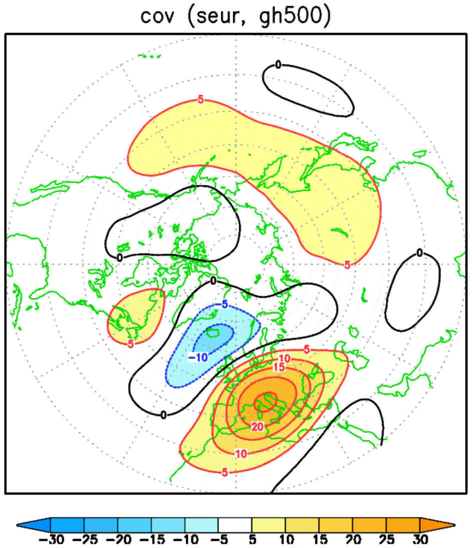

Sub-seasonal variability: the Madden-Julian Oscillation

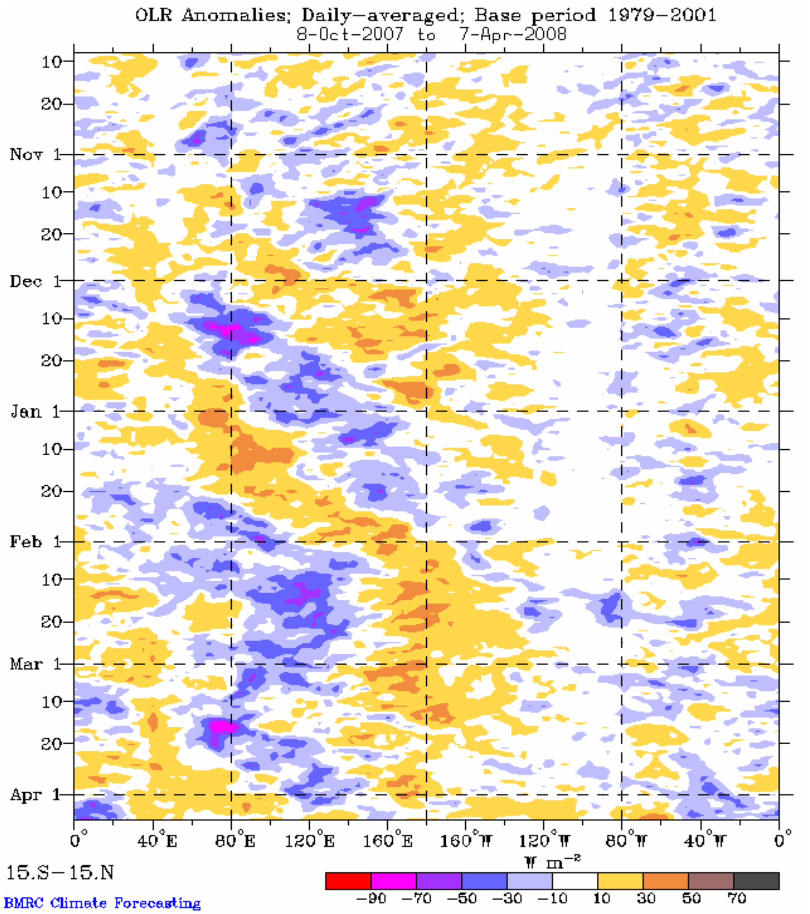

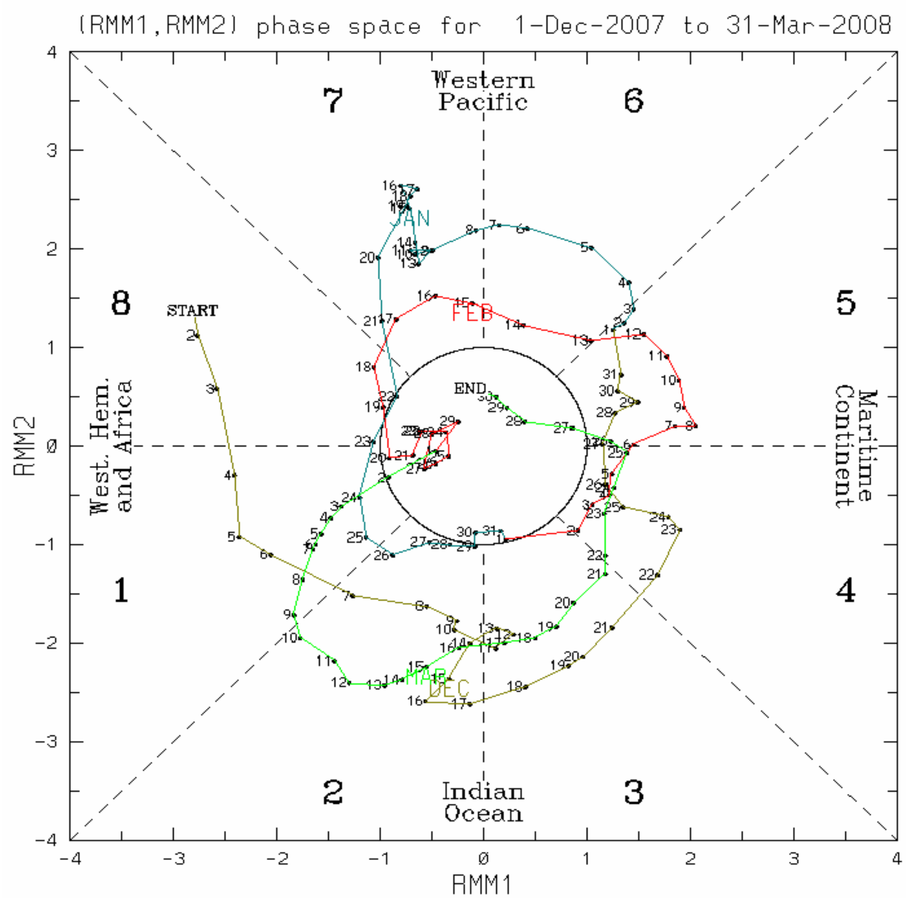

MJO teleconnections in October-March

500 hPa height, MJO phase 3 + 10 days

2002 MOFC hindcasts   2011 MOFC hindcasts   ERA Interim

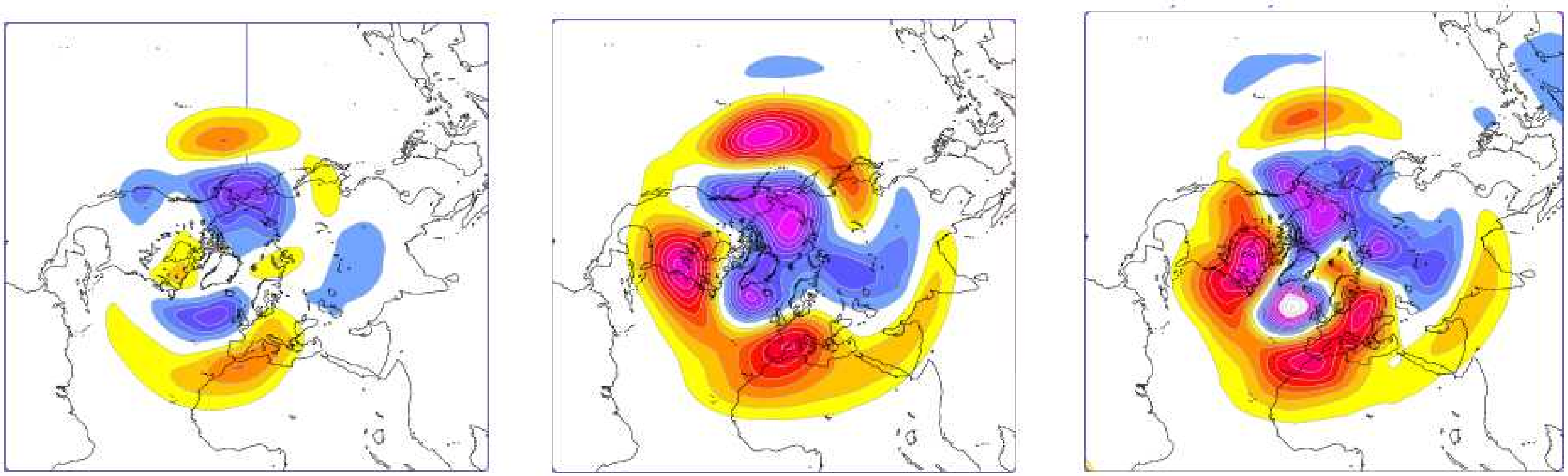

from Vitart 2014

ECMWF monthly fc. for 4-7 Jan. 2010

Z 500 hPa anomaly

Observed anomaly: Mon 20100104 - Sun 20100110

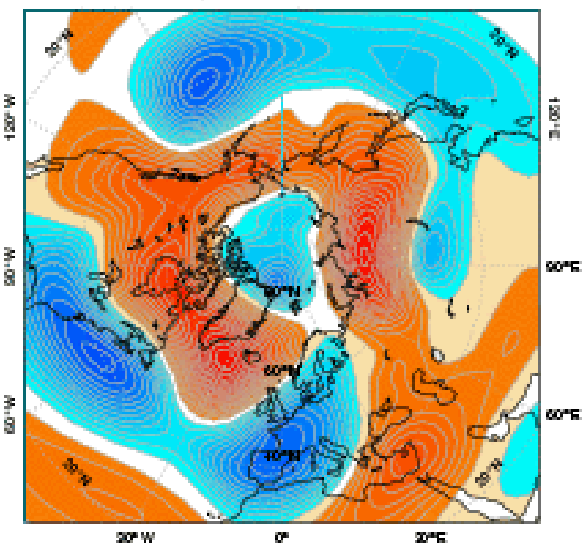

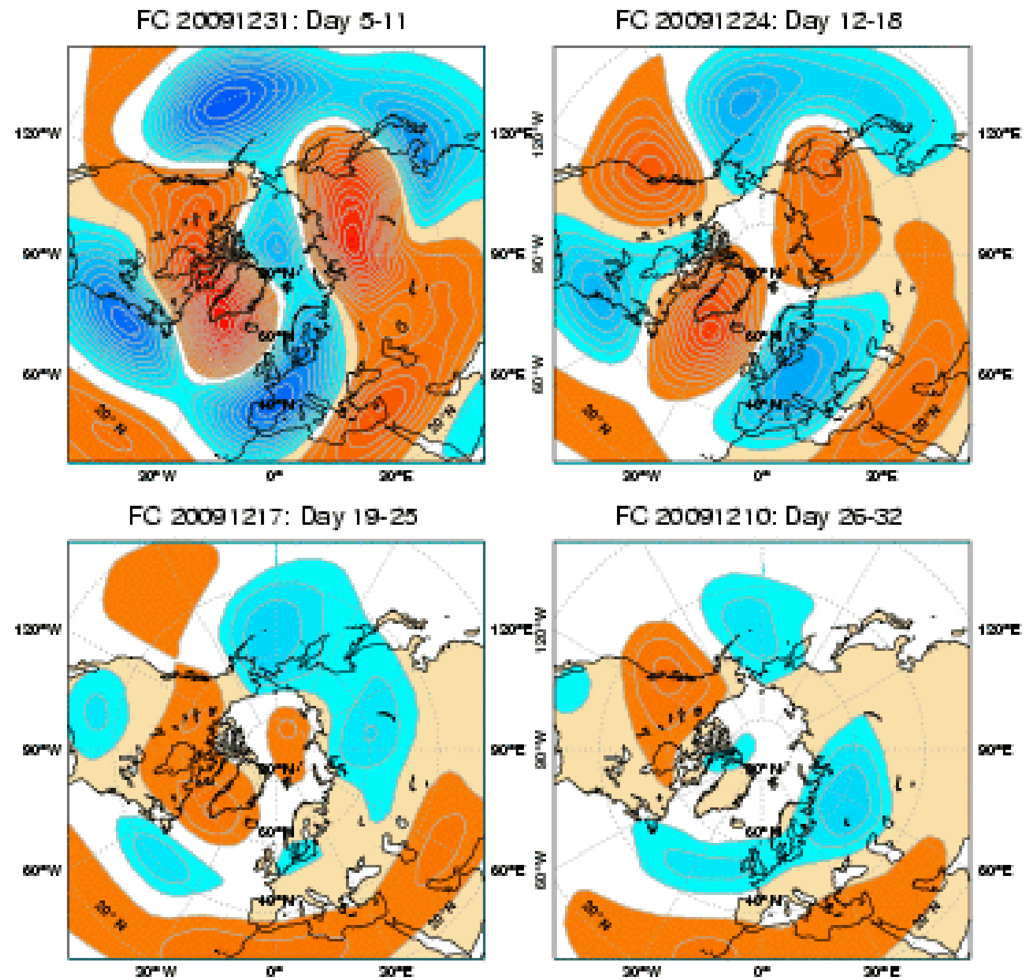

Conclusions

Regional anomalies in atmospheric flow and weather parameters may persist on time scales longer than the deterministic predictability limit, and have substantial societal impacts.

The possibility of performing probabilistic predictions of these events arises from the interaction of the atmospheric flow with slowly varying anomalies in surface conditions, which modify the energy and water sources for the atmosphere.

In the extratropics, persistent anomalies can be generated by (linear) teleconnections with tropical variability (eg ENSO) but also from the alternation of different (non-linear) flow regimes.

Ensemble prediction systems provide an *estimate* of long-range predictability based on the ratio of ensemble spread and ensemble-mean variability.

Predictability over Europe: limited by strong internal variability during winter (but with significant teleconnections on the *sub-seasonal scale*), higher in other seasons when internal variability is reduced.

References

Bjerknes, J., 1969: Atmospheric teleconnections from the Equatorial Pacific. Mon. Wea. Rev., **97,** 163–172.

Charney, J.G. and J.G. DeVore. 1979: Multiple flow equilibria in the atmosphere and blocking. J. Atmos. Sci. **36,** 1205-1216

Horel, J.D. and J.M. Wallace, 1981: Planetary-scale atmospheric phenomena associated with the Southern Oscillation. Mon. Wea. Rev. **109,** 813-829.

Lorenz E.N, 1963: Deterministic nonperiodic flow. J. Atmos. Sci. **20,** 130-141.

Molteni, F., T. Stockdale, M. Balmaseda, G. Balsamo, R. Buizza, L. Ferranti, L. Magnusson, K. Mogensen, T. Palmer and F. Vitart, 2011: The new ECMWF seasonal forecast system (System 4). ECMWF Tech. Memorandum no. 656.

Saji, N.H, B.N. Goswami, P. N. Vinayachandran and T. Yamagata, 1999: A dipole mode in the tropical Indian Ocean. Nature **401,** 360-363.

Trenberth K.E., J.T. Fasullo and J. Kiehl, 2009: Earth's global energy budget. Bull. Amer. Meteor. Soc., **90,** 311-323.

Van Loon, H. and J.C. Rogers, 1978: The seesaw in winter temperatures between Greenland and Northern Europe. Part I: General description. Mon. Wea. Rev. **106,** 296-310.

Vitart, F., 2014: Evolution of ECMWF sub-seasonal forecast skill scores. Q.J.R. Meteorol. Soc.. doi: 10.1002/qj.2256

Walker, G.T. and E.W. Bliss, 1932. World Weather V, Memoirs of the Royal Meteorological Society, **4,** (36) , 53-84.

Wallace, J.M. and D.S. Gutzler, 1981: Teleconnections in the geopotential height field during the Northern Hemisphere winter. Mon. Wea. Rev. **109,** 784-812.

Webster, P.J., A.M. Moore, J.P. Loschnigg and R.R. Leben, 1999: Coupled ocean–atmosphere dynamics in the Indian Ocean during 1997–98. Nature **401,** 356-360.

Wheeler, M.C. and H. H. Hendon, 2004: An all-season real-time multivariate MJO index: Development of an index for monitoring and prediction. Mon. Wea. Rev. **132,** 1917-1932